

MuSCAT3 Release Notes

Daniel Harbeck, Nikolaus Volgenau, Norio Narita, Akihiko Fukui, Mark Bowman, Mark Elphick, JD Armstrong, Jacqueline Han, Jon Nation, Elisabeth Heinrich-Josties, Steve Foale, Matt Daily, Curtis McCully, Annie Kirby, Cary Smith, Brian Haworth, Lisa Storrie-Lombardi, Patrick Conway, Joey Chatelain, Etienne Bachelet, Marshall Johnson, Markus Rabus, Fernando Rios, Sarah Rettinger, Wayne Rosing

Updated November 16, 2020

This document outlines the performance of the MuSCAT3 instrument at the time of its first release to the LCO community. The information herein will allow new MuSCAT3 users to ramp up their science programs. MuSCAT3 users should diligently evaluate their data and adjust the setup of their observations accordingly.

MuSCAT3 is not only a new instrument, but as a multi-channel imager it is also a new *type* of instrument at LCO. The LCO operations team will learn how to maintain MuSCAT3 as the LCO user community learns how to use it. Users should provide feedback or ask questions via science-support@lco.global.

Overall, MuSCAT3 is performing well. However, full characterisation is not complete, and there remain a few loose ends that will be addressed over the next couple of months. (See the Limitations section below.) Some operational interruptions will be necessary when we make improvements.

Data Processing & Format

MuSCAT3 images are processed by the BANZAI pipeline. Standard CCD calibrations such as bias, dark, and sky flat fields are acquired by the observatory for use in BANZAI processing. Calibrations are available in the science archive. Flat fields in the two readout modes (see below) are acquired during morning and evening twilight on alternating nights.

Images from each of MuSCAT3's four channels are stored in individual FITS files. Image names follow the typical LCO name convention, e.g. `ogg2m001-ep02-20201023-0157-e91.fits.fz`. The camera codes for the four MuSCAT3 channels are:

g': ep04
r': ep02
i': ep03
zs: ep01

The image numbers increment independently for each channel. Users should not expect the first image (in a series of exposures) from each channel to have identical image numbers.

Detector performance

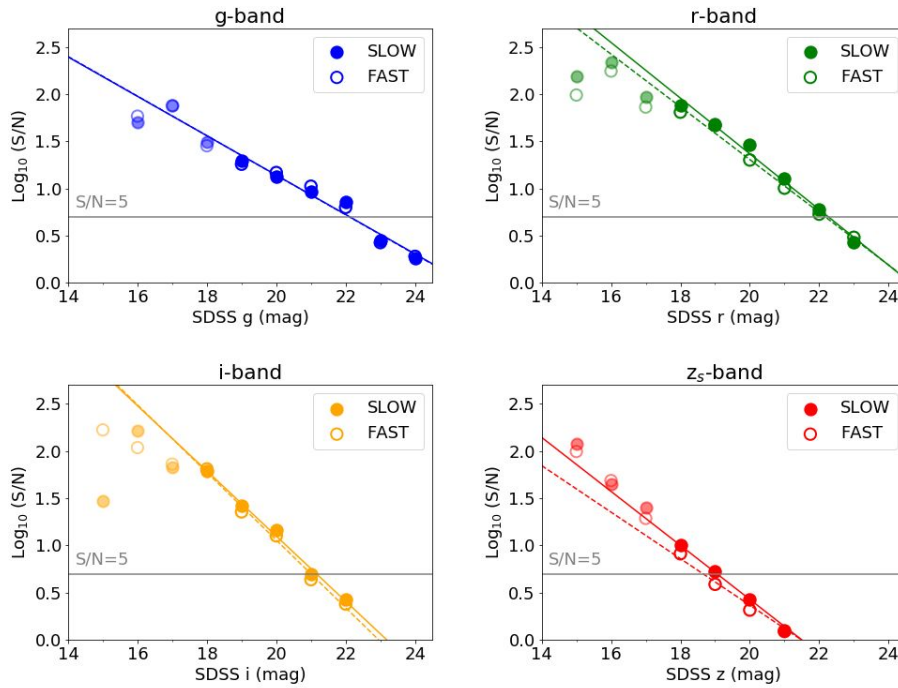
MuSCAT3 supports FAST and SLOW CCD readout modes. The readout overheads are 6 seconds and 46 seconds, respectively. The CCD readout mode is set for all four channels simultaneously. The read noise and full well of the cameras in the different readout modes are given in the table below:

Passband	Read Noise [e-] FAST / SLOW mode	Full well [ke-]	Gain [e-/ADU]
g'	12 / 3.5	120	1.9
r'	12 / 3.5	120	1.88
i'	12 / 3.5	82	1.8
zs	15 / 3.5	71	1.7

Photometric Performance

The *photometric zero points* of MuSCAT3 were estimated from science validation observations. For MuSCAT3's four channels, the zero point offsets relative to the Spectral camera that it replaced are: g': +0.5 mag; r': +0.1 mag; i': -0.15 mag; z': -0.2 mag.

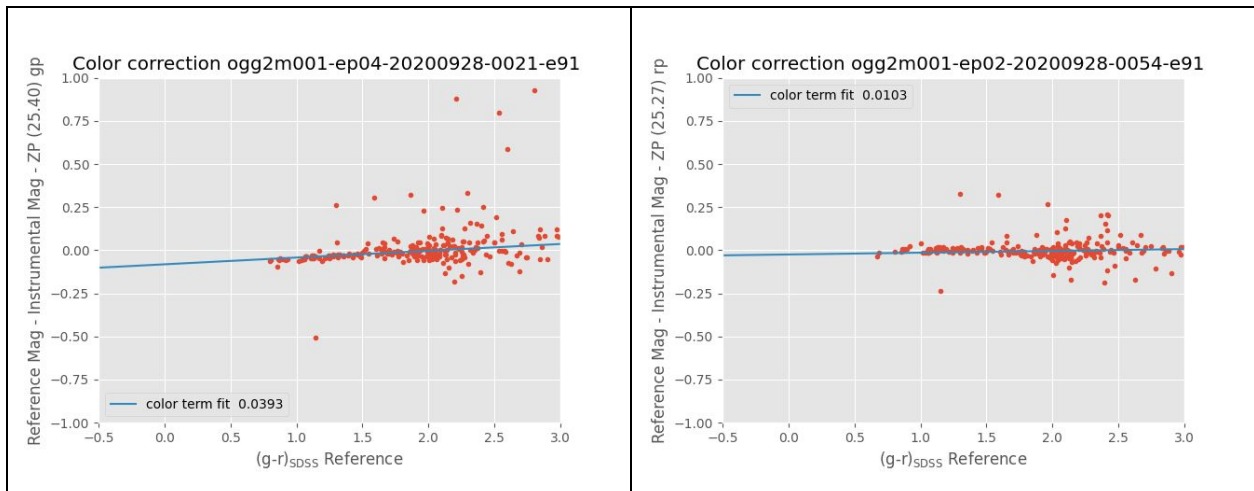
The limiting (S/N=5) magnitudes at airmass 1.3 for a 10 minute exposure in the SLOW / FAST readout mode are, respectively: g': 22.1 / 22.1 mag; r': 22.3 / 22.2 mag; i': 21.2 / 21.0 mag; z': 19.1 / 18.7 mag. These limiting magnitudes differ from the results produced by the LCO exposure time calculator, and users are advised to independently verify that their data meet their expectations. The calculator is being updated; it currently assumes 100% transparency.

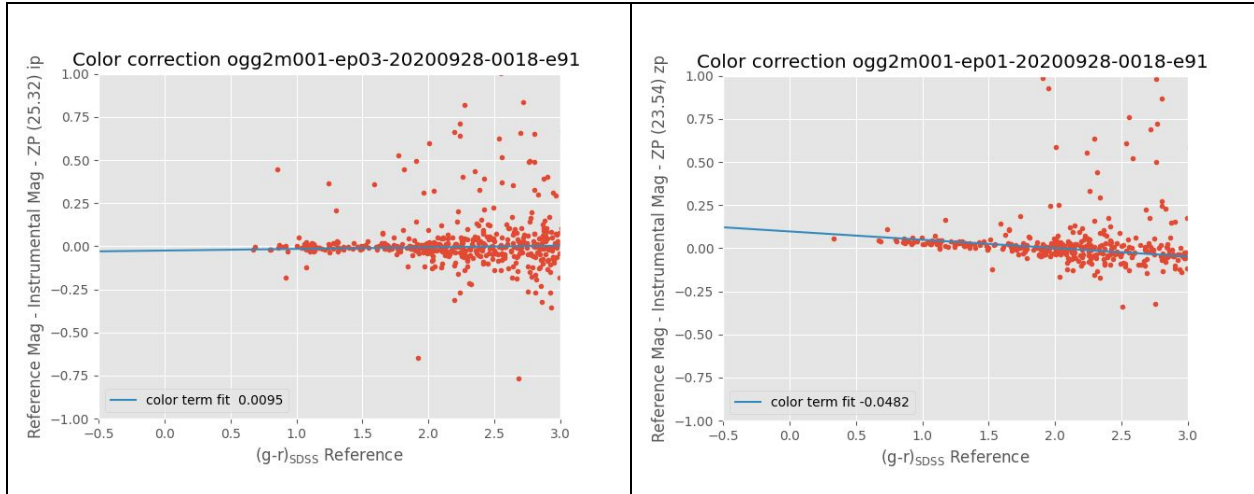


Note: The z_s channel generates a noticeable fringe pattern. The sensitivity in the z_s channel will increase when the camera is replaced with a better fringe-suppressing and higher quantum-efficiency camera. (See Limitations section below.)

Color terms

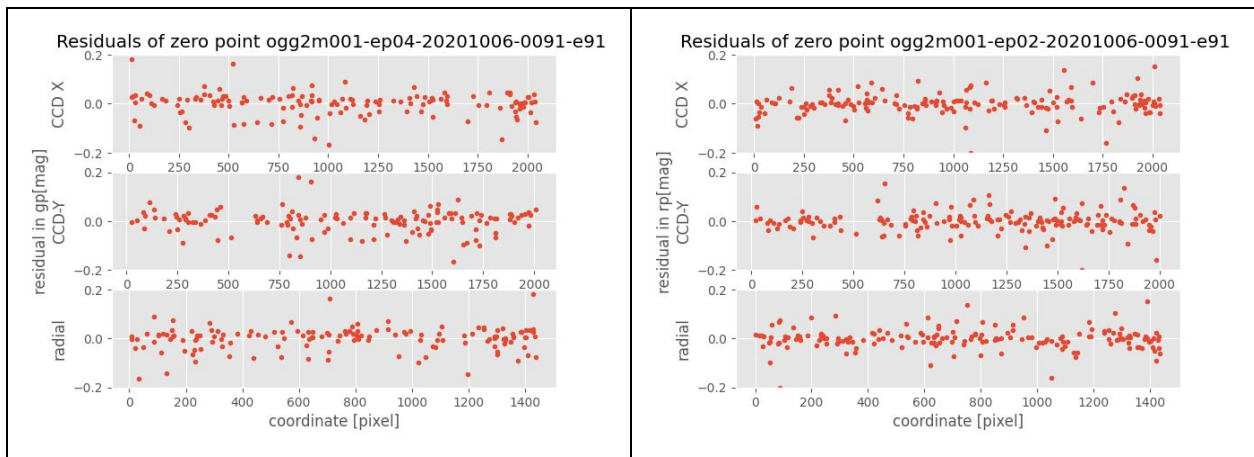
The instrumental *color terms* are represented in the figure below as a correction versus the SDSS reference color in $g'-r'$. Users should expect to color-correct photometry at least in the g' and z_s bands according to their program's needs.

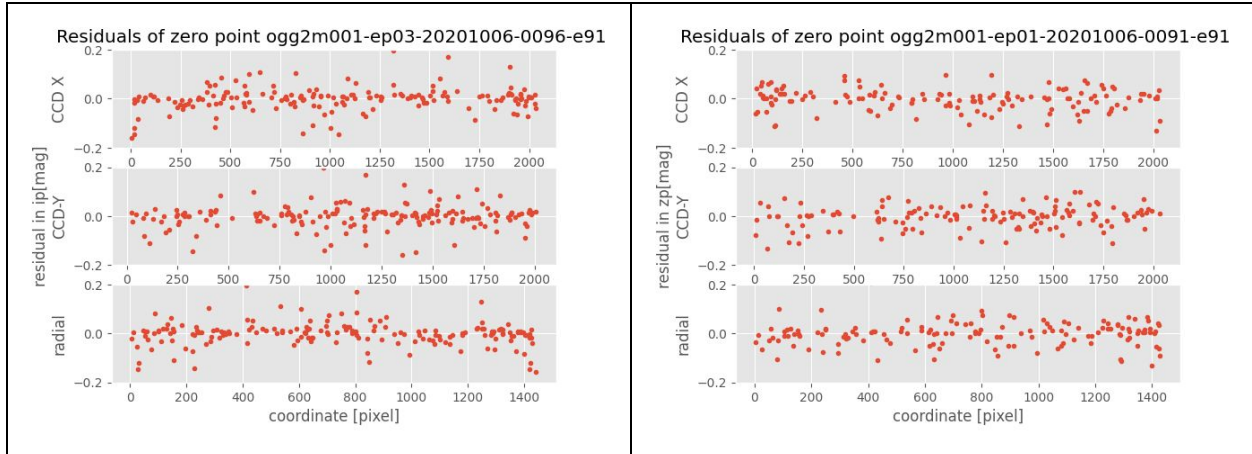




Homogeneity over the field of view

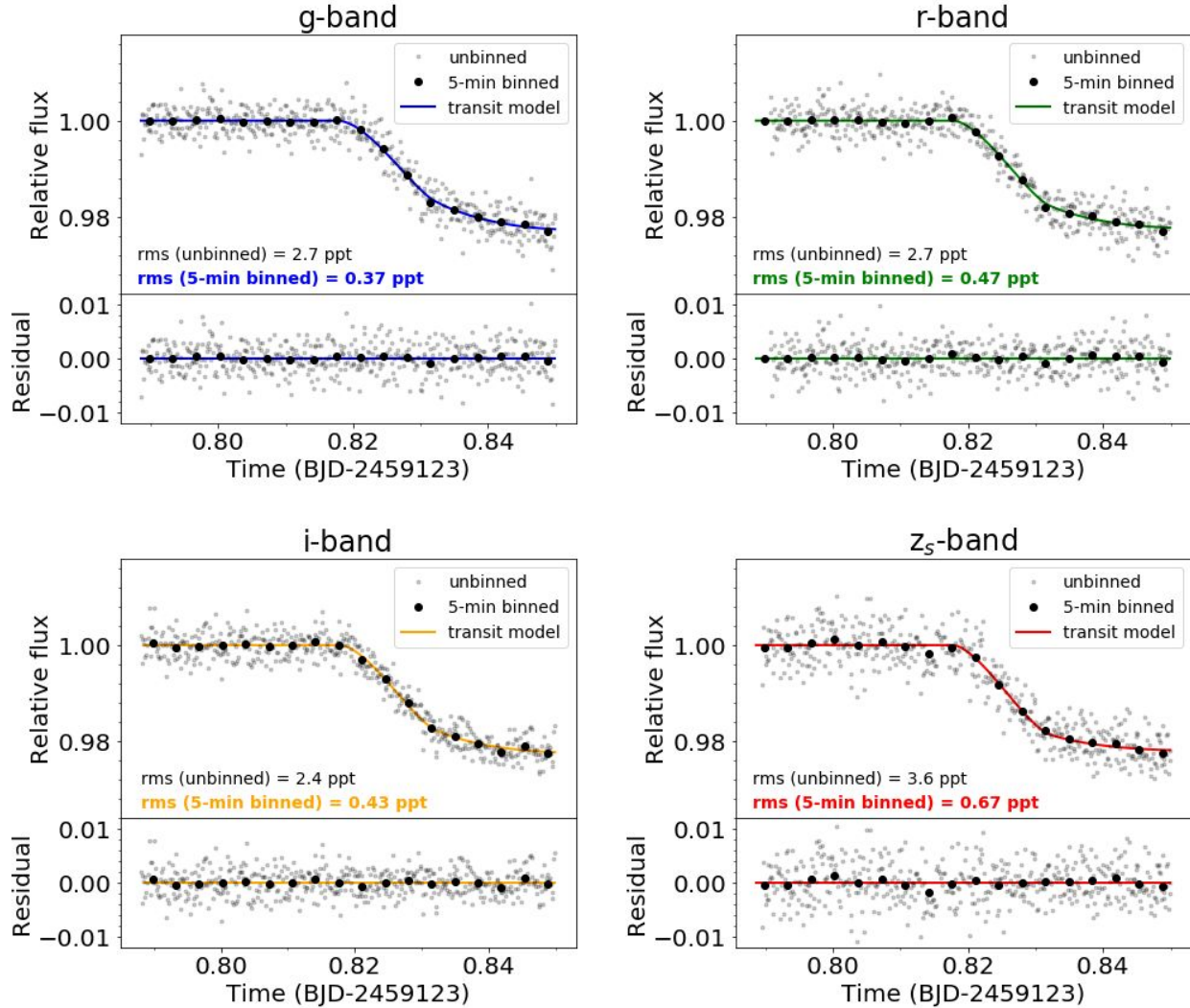
There is currently no evidence of significant photometric zeropoint shifts over the field of view. The following graphs exemplify the residual of the color corrected zeropoint plotted as a function of the x, y coordinates, as well as the radial distance from the detector center. Independent analysis of other observations yielded similar results on homogeneity.





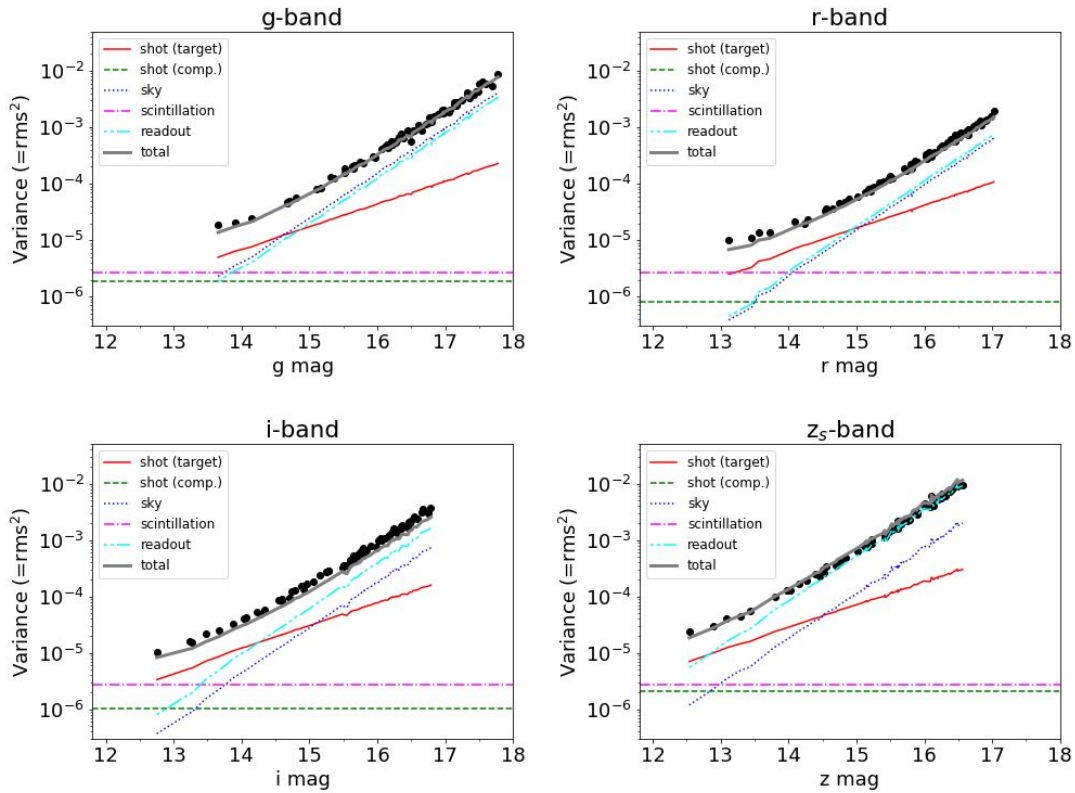
Demonstration of time series photometry

One of the key motivations of MuSCAT3 is observing time-variable objects, such as transiting planetary systems, for several hours within one night. To demonstrate the achievable photometric precision with MuSCAT3, we observed a transit of Qatar-1b, a known Jovian-sized planet orbiting a K dwarf with magnitudes of $g=13.4$, $r=12.7$, $i=12.3$, and $z=12.1$, on October 1, 2020 UT. The target field was observed with exposure times of 5 seconds and the FAST readout mode for all bands. The focus offset was +2 mm. Only the transit ingress was observed for technical reasons. Telescope guiding was not operational during the observation (see Limitations section), resulting in significant displacements of stellar positions on the detectors over the 90-minute-long observation (by ~ 30 pixels in both X and Y directions due to the telescope tracking drifts).



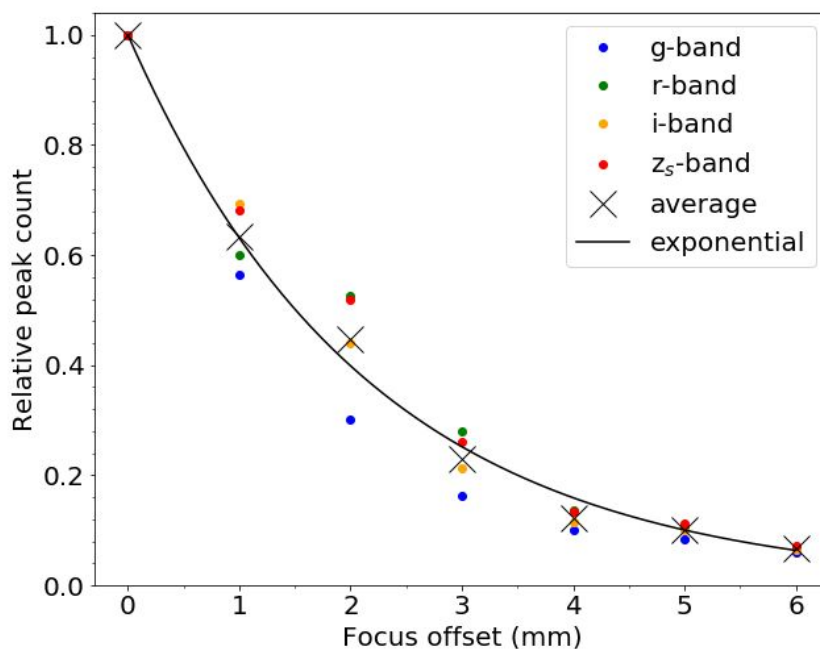
The above light curves were produced by aperture photometry with an aperture size of 12 pixels (3.2 arcsec). Several comparison stars with similar brightness to the target star were used for the relative photometry. The achieved photometric precisions, i.e., rms of the residuals from a transit-model fit, were 2.7, 2.7, 2.4, and 3.6 ppt per exposure, and 0.37, 0.47, 0.43, and 0.67 ppt per 5 minutes, for g, r, i, and z_s bands, respectively.

We also measured the photometric precisions (rms) of dozens of non-variable stars in the same field as Qatar-1. A single non-variable star with a similar brightness to Qatar-1 was used as a comparison star. As shown in the following figure, the measured light-curve dispersions can be explained by the sum of the known errors, i.e., shot noises of the target and comparison stars, sky background noise, readout noise, and scintillation noise. This result demonstrates that the contributions from systematic (unknown) noises are negligible, even without guiding, at least for the magnitude range demonstrated here.



Relation between focus value and peak count

MuSCAT users may want to defocus to avoid saturation and/or to achieve higher photometric precision for bright targets. The relation between the focus offset and the stellar peak count was investigated by imaging targets at airmass=1.1 on a night when the natural seeing was $\sim 0.8''$, as shown in the plot below. Note that the data for 0 offset could not be obtained under the same sky conditions, and the peak count for 0 offset was estimated using a Moffat function with FWHM of $0.8''$. The peak count decays roughly as an exponential function with $\exp(-0.46 \times [\text{focus (mm)}])$. You can find more information about the relation between focus value and peak count from Akihiko Fukui's [MuSCAT3 peak count estimator](#).



Limitations at time of first release (November 2020)

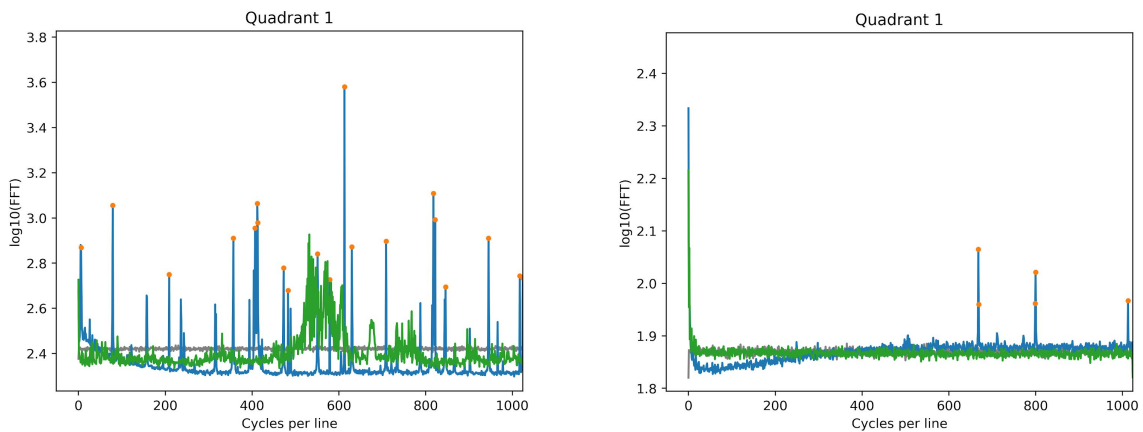
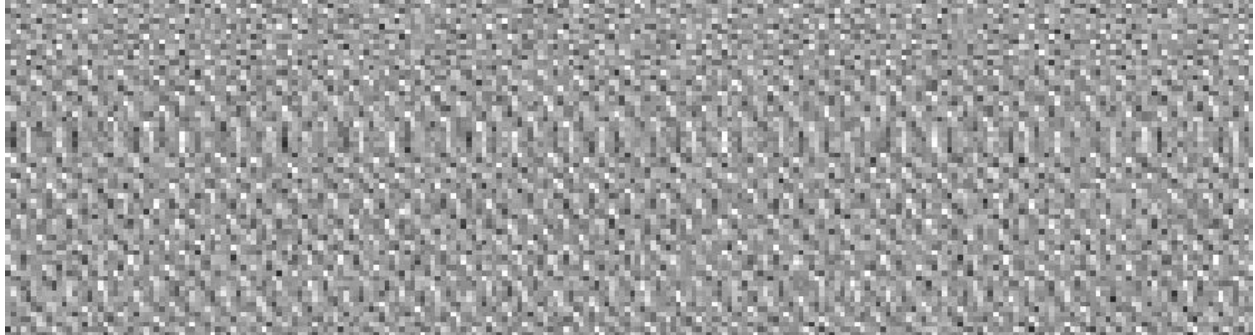
z' band cameras

MuSCAT3 was designed with a Princeton Instruments Sophia 2048BR camera for the z_s channel. This camera confers the benefit of an improved red response and fringe suppression relative to the Pixis cameras used in the g', r', i' channels. However, because of a software bug in the Princeton Instruments' USB driver, the Sophia camera cannot yet be used in a production environment. Until Princeton Instruments releases a new version of their driver, a loaner Pixis 2048B camera is installed in the z_s channel. The Pixis 2048B loaner has lower sensitivity and an elevated read noise (~15 e⁻, rather than 12e⁻, and increased pattern noise).

The date for the release of the new USB3 driver, and hence the conversion to the Sophia camera, has not been set.

Pattern noise

All cameras show elevated pattern noise when the FAST readout mode is used. The source of noise is under investigation, but it may be an inherent feature of the Pixis camera fast readout mode.



Top: Pattern noise is visible in this zoom-in into a bias frame, acquired in the FAST readout mode. The power spectrum (blue: x-direction, green: y-direction) of a bias (ep02) taken in the FAST readout mode (lower left) illustrates the pattern noise. The power spectrum of the SLOW readout mode (lower right) is very clean. The read noise is 12 and 3.5 electrons, respectively, but note that in the FAST readout more, the noise is non-gaussian.

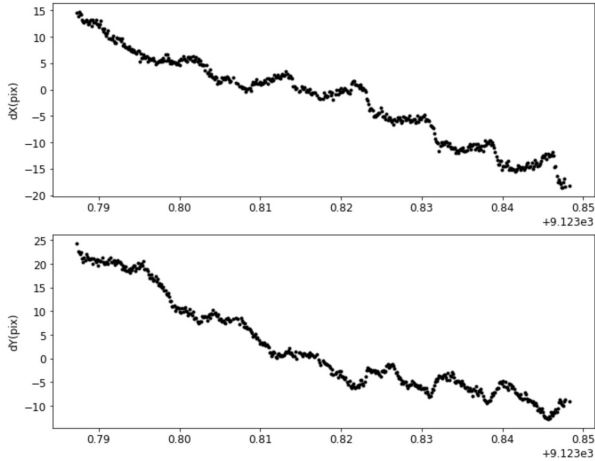
Diffusers

The MuSCAT3 design calls for photonic diffusers that can expand the point spread function to an 11" diameter top-hat profile. However, because of mechanical problems with the motorized stages that control diffuser insertion, the diffusers have been removed from MuSCAT3 and cannot be selected for observations. The time scale for diagnosing the problem with the stages and re-installing the diffusers is unknown.

Telescope tracking

During commissioning observations two deficiencies in the telescope have resurfaced. The telescope's pointing drifts during unguided observations, and on short time scales, the pointing

can jump by up to 2 arcseconds. Because shutter opening times are not synchronized with the tracking cycle, any exposure can be affected by the jumps, although longer exposures are more likely to span a jump than shorter exposures.



Reference star x/y positions during an open-loop tracked planet transit observation. Note the cyclic, sudden jumps in the telescope position.

To preserve image quality, MuSCAT3 observations should be guided. With the decommissioning of the Spectral camera, the 4AG autoguider unit was removed from the telescope. In its place, an inventoried facility guider was installed and restored to service. Test observations demonstrated that the tracking errors were successfully suppressed when the facility guider was active. The default MuSCAT3 observing mode uses guider images with 5 second exposures. **Note:** Tests of the facility guider will continue after MuSCAT3 is released for general science observations.

Field rotation

The (de)rotator on the 2m telescope has an azimuth range slightly greater than one full rotation. For most sky positions, only one derotator position is possible. Consequently, long-duration observations, such as the monitoring of an exoplanet transit, may be terminated when the derotator hits a limit. The derotator limits of the 2m telescope are described in Appendix D of the [“Getting Started” guide](#). We recommend that long-duration observations be broken down into sub-observations, so that the derotator can “unwrap”.

Acknowledgement of MuSCAT3

All papers based on MUSCAT3 data shall contain the following acknowledgement:

“This paper is based on observations made with the MuSCAT3 instrument, developed by the Astrobiology Center and under financial supports by JSPS KAKENHI (JP18H05439) and JST PRESTO (JPMJPR1775), at Faulkes Telescope North on Maui, HI, operated by the Las Cumbres Observatory.”

Relevant links

- [Overview of the MuSCAT3 instrument](#) (updated 4 Nov 2020)
- [Getting Started with MUSCAT API & Portal Requests](#)
- List of [Commissioning and Science Validation Data](#)

Transition-to-operations Timeline

Pre-installation assembly begins: 14 Sep 2020

Installation on Faulkes Telescope North: 27 Sep 2020

First light; engineering commissioning begins: 28 Sep 2020

First science observation: 1 Oct 2020

Observations for science validation projects begin: 8 Oct 2020

Release for routine science observations: 4 Nov 2020

Acknowledgements:

- Photometry comparisons are made to “The ATLAS All-Sky Stellar Reference Catalog”
Tonry, J.L., Denneau, L., Flewelling, H., et al. 2018, ApJ, 867, 105.
doi:10.3847/1538-4357/aae386